

PAPER • OPEN ACCESS

Determination of Mechanical Characteristics Plasma Hardened Wheel Steel

To cite this article: A V Bogomolov *et al* 2020 *IOP Conf. Ser.: Mater. Sci. Eng.* **969** 012037

View the [article online](#) for updates and enhancements.

You may also like

- [Investigation of the nanoscale elastic recovery of a polymer using an atomic force microscopy-based method](#)
Yanquan Geng, Yongda Yan, Zhenjiang Hu et al.
- [Micromachined contactless pin-flange adapter for robust high-frequency measurements](#)
S Rahiminejad, E Pucci, S Haasl et al.
- [Elastic-plastic deformation of single-crystal silicon in nano-cutting by a single-tip tool](#)
Ning Huang, Ying Yan, Ping Zhou et al.



ECS The Electrochemical Society
Advancing solid state & electrochemical science & technology

242nd ECS Meeting

Oct 9 – 13, 2022 • Atlanta, GA, US

Early hotel & registration pricing ends September 12

Presenting more than 2,400 technical abstracts in 50 symposia

The meeting for industry & researchers in

BATTERIES
ENERGY TECHNOLOGY
SENSORS AND MORE!

 Register now!

  **ECS Plenary Lecture featuring M. Stanley Whittingham,**
Binghamton University
Nobel Laureate –
2019 Nobel Prize in Chemistry



Determination of Mechanical Characteristics Plasma Hardened Wheel Steel

A V Bogomolov¹, A T Kanaev² and T E Sarsembaeva²

¹S. Toraighyrov Pavlodar State University, 64, Lomov Street, Pavlodar, 140008, Kazakhstan

²L. N. Gumilyov Eurasia National University, 2, Satpayev Street, Nur-Sultan, 010008, Kazakhstan

E-mail: bogomolov71@mail.ru

Abstract. A technique for measuring the mechanical properties of plasma-hardened wheel steel with nanoindentation is applied. The purpose of the work is to demonstrate and substantiate the serious differences between the mechanical properties and behavior of materials in nano-volumes from those obtained in traditional macroscopic tests. The features of measuring mechanical properties – hardness, Young's modulus, elastic recovery – affecting the wear resistance of the surface layers of the material are given. Measurement of the physic mechanical properties of the material makes it possible to evaluate and select the optimal technology for surface modification by surface plasma hardening. It is noticed that the objectivity of determining the hardness, elastic modulus, elastic recovery and flow stress depends on the parameters of the measuring equipment used and strict adherence to the requirements for the imprint depth depending on the thickness of the hardened layer. The studies carried out on wheel steel samples from the rim and from the ridge of a railway wheel subjected to surface plasma hardening under the same conditions. The HV and H of the wheel rim are greater than the corresponding values of the flange, and the young modulus of the wheel flange, on the contrary, is greater for the flange.

1. Introduction

Reliability and durability of machine parts and mechanisms operating under conditions of friction and wear, in many cases, is ensured by increasing the hardness of the surface layer. Under real operating conditions, minimization of wear depends on the elasticity and resistance to deformation of the surface layer not less than on hardness [1–5]. These properties are determined by the basic physical and mechanical characteristics of the surface layer, namely, hardness, elastic modulus and elastic recovery. These parameters are measured using instrumental indentation (nanoindentation) according to GOST R 8.748-2011 (ISO 14577-1: 2015), and their change is possible by surface modification, for example, by plasma hardening.

With the advent and development of the continuous measurement nanoindentation method, it became possible to quantify some important characteristics of metallic materials within individual submicroscopic zones, in particular, Vickers hardness, Young's modulus, flow stress, etc. Thus, in [6], nanoindentation aluminum alloys measured the submicrocrystalline hardness.

Speaking about the physical nature of nanohardness, it should be said that, despite the increased amount of information obtained by nanoindentation, the physical justification of micromechanisms of



hardness remains poorly satisfactory. So, an example of the insufficiency of existing ideas about the nature of hardness is the problem of explaining the reasons for the large-scale size factor, which manifests itself in an increase in the number of hardness with a decrease in the load and dimensions of the print, especially at depths $h < 1 \mu\text{m}$. An explanation of the reasons for the size factor by the dislocation plasticity mechanism by introducing the required number of dislocations did not lead to a resolution of the problem [7–9]. Formally, it is possible to introduce the required number of dislocations into the material under study, however, their density at $h < 100 \text{ nm}$ becomes unrealistically large ($> 10^{14} \text{ sm}^{-2}$). In addition, this contradicts the results of microstructural studies, which do not detect such a number of dislocations. Obviously, the mechanical properties and behavior of materials in nano-volumes can, for a number of reasons, differ greatly from those obtained in traditional macroscopic tests, since with the decrease in the size of the loaded region by many orders of magnitude, many new factors begin to affect the material properties. The localization of the load leads to a strong hardening of the material in the deformation zone and the resulting large stress gradients can strongly affect the mechanisms of plastic flow. Therefore, it is not clear in which direction the material moves from under the indenter. It is believed that in plastic materials the material flows from under the indenter towards the free surface. In fact, mass transfer is directed into the volume, which compacts the material in the zone of local deformation [10–12].

Currently, there is a lot of direct evidence of the growing role of nonequilibrium point defects in mass transfer with a decrease in the size of the contact spot. There is also convincing evidence of a significant change in the structure of materials under the indenter because of amorphization, phase transformations, and the formation of a nanocrystalline structure. However, in existing theories of hardness proceeding from dislocation mechanisms of plastic deformation, these circumstances are not taken into account and are not explained [13–16].

In addition to all this, due to the small size of the deformed region ($\sim h$), large relative strain rates $\epsilon \sim v/h$ is realized even at small absolute penetration rates - v . As a result, the nanoscale hardness of a material can be two or more orders of magnitude higher than the yield strength. This implies the need to justify physical ideas about the nature of hardness, in general, and nanohardness, in particular.

Experimental studies show that when working out the optimal regimes of plasma hardening, it is necessary to ensure a smooth change in structure and microhardness in depth. The solution to this problem is facilitated by the use of the nanoindentation method when studying the physic mechanical properties of plasma-hardened steel wheels.

2. Object and research methods

In this work, the measurement of some mechanical characteristics of wheel steel subjected to surface plasma hardening was carried out using the UPNN-170 installation of the PlazmaCenter scientific and production company (St. Petersburg).

Technical characteristics of the UPNN-170 installation: rated current – 120 A, rated operating voltage – not more than 42 V, argon consumption 5 l/min, cooling water consumption 180–220 l/h. Hardness was measured by nanoindentation at the Center for the Study of Material Properties of Tomsk Polytechnic University.

Wheel steel is represented by two samples: sample No. 1 is cut from the rim, and sample No. 2 is from the crest of a railway wheel subjected to surface plasma hardening under the same conditions.

Samples for research with dimensions of 20x30 mm were subjected to grinding and polishing on a LaboPol-5 machine. Because of electrochemical polishing, the height of surface irregularities did not exceed 10 nm. Processing and analysis of the obtained surface images was carried out using Nova software. During the experiment, a probe sensor of the SPMProdeNSC 15/AIBS type was used. The Vickers hardness thus determined is equal to the average pressure on the contact surface of the “indenter-sample”. The hardness was measured at room temperature under continuous loading with a linearly increasing in time load up to 150 mH.

The loading and unloading of the indenter, as well as the recording of the P-h diagram (applied load and indenter penetration depth) were carried out automatically. This method of measuring hardness,

called the method of kinetic hardness (continuous indentation of an indenter), allows one loading-unloading cycle to determine the depth of unreduced h_{max} and recovered (plastic) h prints, Young's modulus, as well as the work of plastic and elastic deformation during indentation. Figure 1 shows the kinetics of the change in the load P and the penetration depth h of the indenter in the loading – unloading cycle (a) and the diagram of the dependence of the load P on the penetration depth h (b), where P_{max} is the maximum load applied to the sample, h_{max} is the penetration depth of the indenter; h_f – residual area after unloading. A_{pl} and A_{erabot} of plastic and elastic deformation, $tg\alpha$ is the slope of the linear part of the unloading part.

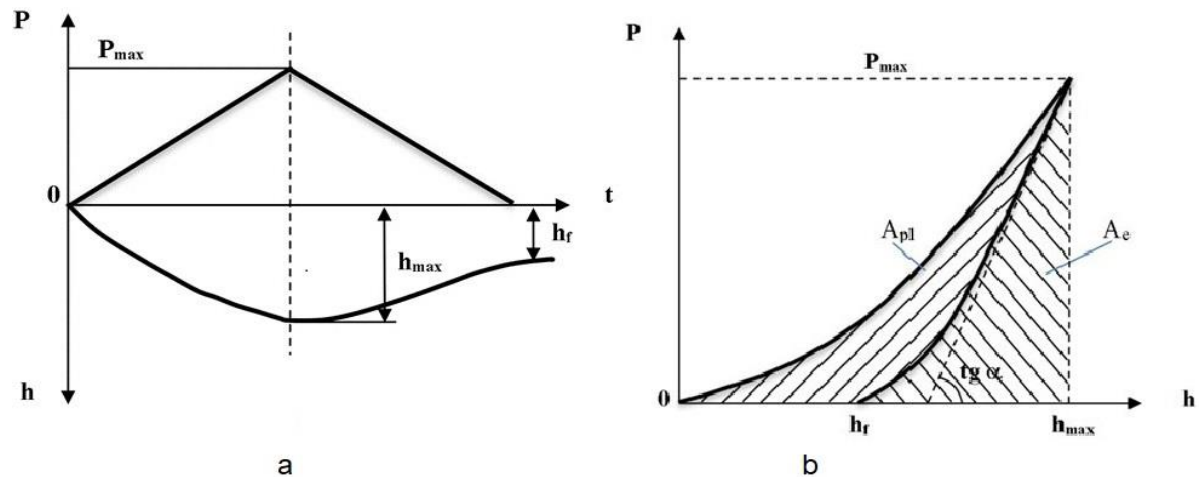


Figure 1. Dependences of the load P and the penetration depth h of the indenter on time t in the loading - unloading cycle (a) and a diagram of the dependence of P on h (b).

The maximum immersion depth of the indenter h_{max} using data from a tapping scanning probe microscopy measured the indenter footprint. The speed of loading and unloading the indenter was 300 mH/min. To process the test results used the method of Oliver and Farr [10].

The nanoindentation method consists in pressing an indenter with a diamond tip, with a load acting on it, into the surface layer of the material under study and determining the thickness of this layer using the software of a nanohardness meter. Processing of experimental data is carried out according to the results of measurements of at least 3 prints obtained under the same experimental conditions. Figure 2 shows the indenter prints in the surface layer of the material at a certain distance from the surface.

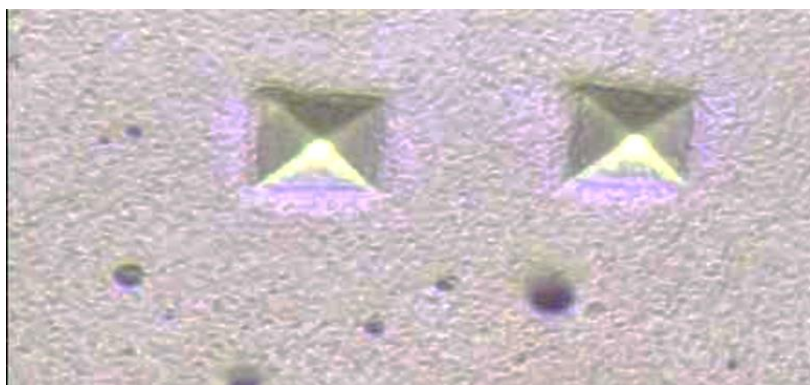


Figure 2. Imprint indenter in the near-surface layer of the material.

The work of the NanoHardness Tester nanosolid hardness tester is that because of passing a current pulse through the coils located in the magnetic field of a permanent magnet, an electric field is created that presses on the indenter with a diamond tip. The indenter drops to a point on the surface of the sample

with a predetermined load. After the load on it has reached its maximum value, and the direction of the current of the coils is changing in the opposite direction, it returns to its original position.

After the load reaches its maximum value, the indenter begins to unload, the load acting on it gradually decreases to zero, and he returns to his original position. In this case, the unloading curve is produced, which shows that upon indentation the sample is deformed elastically elastic, i.e. the material from under the indenter does not return to its former position to the end. The mismatch between the load and unload lines is probably due to inelasticity.

3. Results and discussion

The results of determining the mechanical characteristics of plasma-hardened wheel steel according to are presented respectively in Table 1 for the wheel rim and in Table 2 for the wheel flange. Figure 3 shows one of the experimental loading and unloading curves showing the indentation process on sample No. 1 from the rim of a railway wheel. Similar curves were obtained for sample No. 2 wheel flange.

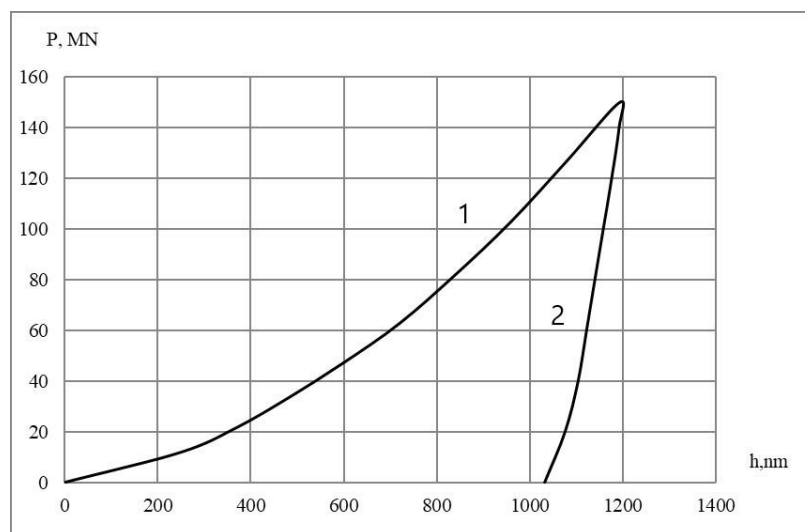


Figure 3. Loading (1) and unloading (2) curves for sample 1.

The plot of diagram 2 (Figure 3) gives information related to the elastic properties of the material; it is caused by the relaxation of energy accumulated during elastoplastic deformation during indenter penetration. The mismatch of curves 1 and 2 indicates the presence of permanent deformation after completion of the indentation procedure.

A comparison of the data in Tables 1 and 2 shows that the HV and H of the wheel rim are larger than the corresponding flange values, and the Young's modulus of the wheel flange, on the contrary, is larger for the flange compared to the rim (231.7–246.8).

The results obtained complement well the data presented by other researchers [17–20].

4. Conclusion

The objectivity of determining hardness, modulus of elasticity and elastic recovery depends on the parameters of the measuring equipment used and strict adherence to the requirements for the depth of the imprint depending on the depth of plasma hardening.

The mechanical properties and behavior of materials in nano-volumes can be very different from those obtained in traditional macroscopic tests, since with a decrease in the size of the loaded region (by many orders of magnitude), many new factors begin to affect the material properties.

The localization of the load leads to a strong hardening of the material in the deformation zone, the large stress gradients arising from this can strongly affect the mechanisms of plastic flow, and the structure of the materials under the indenter can significantly change because of amorphization, phase transformations, and the formation of a nanocrystalline structure.

Table 1. Mechanical characteristics of the wheel rim.

N of experiment	Mechanical characteristics of the wheel rim at 20 μm deviation from the edge of the sample deep into the metal			Mechanical characteristics of the wheel rim at 1700 μm deviation from the edge of the sample deep into the metal		
	HV	H, MPa	E, GPa	HV	H, MPa	E, GPa
1	398.00	4222.86	217.32	466.22	4939.52	254.11
2	385.32	4082.40	226.33	378.08	4005.66	245.44
3	361.22	3827.01	211.70	373.25	3954.54	254.95
4	389.10	4122.39	221.29	354.25	3753.25	245.98
5	358.02	3793.15	229.06	383.95	4067.88	230.76
6	395.26	4187.66	252.30	397.99	4216.62	248.90
7	366.76	3885.80	243.07	385.83	4087.81	230.62
8	386.15	4191.21	235.22	369.62	3916.01	261.58
9	406.59	4307.70	233.89	398.50	4222.04	253.07
10	463.92	3855.66	236.25	386.23	4092.04	251.74
11	366.71	3885.21	242.59	–	–	–
Aver.	388.80	4032.80	231.70	384.38	4072.39	241.41

Table 2. Mechanical characteristics of the wheel flange.

N of experiment	Mechanical characteristics of the wheel flange at 40 μm deviation from the edge of the sample into the metal			Mechanical properties of the wheel flange at 100 μm deviation from the edge of the specimen deep into the metal		
	HV	H, MPa	E, GPa	HV	H, MPa	E, GPa
1	350.74	3715.99	287.72	392.01	4153.16	210.41
2	354.93	3760.39	254.69	356.29	3774.81	210.65
3	334.65	3545.52	219.53	387.87	4109.37	230.99
4	365.16	3568.82	232.74	370.25	3922.27	241.84
5	367.65	3895.16	239.30	375.79	3981.44	247.86
6	–	–	–	366.42	3882.17	337.77
Aver.	354.6	3697.2	246.8	374.77	3323.51	246.59

References

- [1] Firstov S 2008 Establishment of limit values of hardness, elastic deformation and the corresponding stress of materials by the method of automatic indentation *Materials Science* **61** 8 15–21
- [2] Makarov A, Pozdeeva N and Savrai R 2012 Improving the wear resistance of hardened structural steel by nanostructural friction treatment *Friction and wear* **22** 6 444–445
- [3] Gogolinsky K, Lvov N and Useinov A 2017 The use of scanning probe microscopes and nanosolid testers to study the mechanical properties of solid materials at the nanoscale *Factory laboratory, Diagnostics of materials* **73** 6 28–36
- [4] Tsui T, Pharr G and Oliver W 1995 Nanoindentation and Nanoscratching of Hard Carbon Coatings for Magnetic *Materials Research Society* **383**

- [5] Leyland A and Matthews A 2019 On the significance of the H/E ratio in wear control: a nanocomposite coatings approach to optimized tribological behavior *Wear* **246** 1 1–11
- [6] Chikova O, Shishkina E and Petrova A 2014 Measurement by hard nanoindentation of hardness of submicrocrystalline industrial aluminum alloys obtained by dynamic pressing *Physics of Metals and Metallurgy* **115** 5 555–560
- [7] Golovin Yu, Ivolgin V and Korenkov V 2017 Determination of the complex of mechanical properties of materials in nano volumes by nanoindentation methods *Condensed Matter and Interphase Boundaries* **3** 2 122–135
- [8] Goldstein M, Litvinov V and Bronfin B 1986 *Metallophysics of High - Durable Alloys* (Moscow: Metallurgy) p 310
- [9] Sosnin N, Ermakov S and Topolyansky P 2013 *Plasma technology* (St. Petersburg: Publishing House of the Polytechnic University) p 403
- [10] Oliver W and Pharr G 2019 An improved technique for determining hardness and elastic modulus using load and displacement sensing indentation experiments *Journal Materials Research* **7** 6 1564–1583
- [11] Golovin Yu 2008 Nanoindentation and mechanical properties of materials in a nanoscale (review) *FTT* **50** 12 1113–1142
- [12] Kanayev A and Bogomolov A 2018 Increase of wear resistance and contact-fatigue strength of wheel steel by plasma hardening *Solid State Phenomena* **284** 1144–1150
- [13] Kanayev A, Bogomolov A and Sarsembayeva T 2017 Overall hardening of solid-rolled wagon wheels by volume quenching and surface plasma processing *Solid State Phenomena* **265** 706–711
- [14] Rybin V, Malyshevsky V and Khlusova E 2019 Technology for creating structural nanostructured steels *Metallurgy and heat treatment of metals* **648** 6 3–7
- [15] Kozlov E, Popova N and Koneva N 2014 Fragmented structure formed in bcc steels during deformation *Izv. RAS, Physical Series* **68** 10 1419–1427
- [16] Tushinsky L 2004 *Structural theory of structural strength of materials* (Novosibirsk, NSTU Publishing House) p 400
- [17] Urtsev V, Gornostyrev Yu and Kornilov V 2012 Nanoengineering in the steel industry *Steel in translation* **42** 2 130–131
- [18] Cui D, Wang H and Li L 2015 Optimal design of wheel profiles for high-speed trains *Proceedings of the institution of mechanical engineers Part F-Journal of rail and rapid transit* **229** 248–261
- [19] Garnham J, Franklin F and Fletcher D 2007 Predicting the life of steel rails *Proceedings of the institution of mechanical engineers, Part F-Journal of rail and rapid transit* **221** 45–58
- [20] Pandkar A, Arakere N and Subhash G 2015 Ratcheting-based microstructure-sensitive modeling of the cyclic hardening response of case-hardened bearing steels subject to Rolling Contact Fatigue *International journal of fatigue* **73** 119–131